WEMPEC

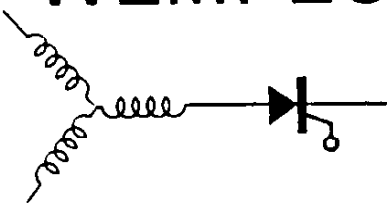

Wisconsin Electric Machines and Power Electronics Consortium

RESEARCH REPORT
82-13

Saturation Effects in the Stability Analysis of a VSI Induction Motor Drive

Yi-Kang He and T.A. Lipo
University of Wisconsin
Madison, Wisconsin, U.S.A.

Department of Electrical and Computer Engineering
University of Wisconsin-Madison
Madison, Wisconsin 53706

December 1982

Paper
UDC 621.313.333.016.352 : {621.314.57 : 621.311.69}

Saturation Effects in the Stability Analysis of a VSI Induction Motor Drive

By

Yi-Kang He Non-member T. A. Lipo Non-member

Summary

A computer model of a saturated induction mcchine is introduced which takes into account the effect of spatially dependent main-flux saturation. The approach is used to model a voltage source inverter (VSI) drive and the instability region of such a drive system is predicted with the new saturation model. Comparison of the results computed by the new model with both tested results and computed results predicted by the conventional quasi-linear model indicate surprisingly important effects of saturation on the small as well as large signal behavior (transients) of a drive system. Discrepancies which have long existed between theory and practice concerning the prediction of dynamic instability of VSI drive by the small signal theory are resolved.

1. Introduction

Due to its widespread application the voltage source inverter (VSI) fed induction motor drive is a very important class of AC frequency variable drive. Since a stepped wave voltage is supplied to the motor there are many new features and corresponding new problems associated with this type of drive. One important such problem is the instability that occurs at low frequency due to the interchange of energy between its DC link filter components and magnetic field and rotor of the machine. Many application opportunities demand operation over a wide speed range, particularly low speed operation. Therefore, the problem of system instability at low operating frequencies is a major concern in the design of VSI induction motor drive.

In the past, considerable work has been devoted to the analysis of VSI drives and models have been developed to predict dynamic behavior[1][2]. These models have been successfully used to predict the instability phenomenon of a drive system and to identify the trend of the instability region with changes in system parameters. However, there is no denying the fact that in some cases the theoretical prediction still does not correlate well with practical measurements. In general, it has been observed that the predicted instability region is usually larger than the measurement and the added damping has been attributed to inverter losses which are not included in the usual analysis[3]. Instability is typically predicted to occur over a range of no load conditions and to persist up to a particular load condition. The predicted instability region takes on the form of a half-oval with the widest portion of the instability range occuring at no load[1]. On the other hand, test results often indicate that the no load condition is stable and the motor must be loaded before instability can occur[3]. Oscillations begin to appear as the load is increased and are sustained over a range of load. When the load is increased beyond a certain point the amplitude of the oscillation is observed to decrease until at heavy load the oscillation again disappears. It appears that this phenomenon cannot be predicted by classical models even with conventional models of saturation.

Recently, however, a new small signal computer model of a saturated induction machine has been developed which takes into consideration the spatial dependence on main flux saturation[4]. The authors have extended this model to portray large signal transients as well a small signal dynamics[5]. Using this new model, the instability region obtained by inserting additional resistances in series with stator of

Yi-Kang He was & *T. A. Lipo* is with Departmemt of Electrical and Computer Engineering, University of Wisconsin-Madison, U. S. A. Manuscript received Feb., 17, 1983.

sinusoidally excited induction machine was predicted with extraordinary accuracy. The purpose of this paper is to extend this new analytical model to the study of induction motor drives and, in particular, to improve the prediction of the instability region for a VSI induction motor drive system.

2. Concept of Transient Saturation

In order to illustrate the concept of transient saturation and its influence on stability, a typical magnetizing characteristic of an induction machine is shown in Fig. 1. Along this magnetizing characteristic, three magnetizing reactances can be defined, namely

Unsaturated magnetizing reactance:

$x_{m(unsat)}=\tan(\alpha_0)$

Steady state saturated magnetizing reactance:

$x_{m(sat)}=\tan(\alpha_s)$

Transient saturated magnetizing reactance:

$x_{mt(sat)}=\tan(\alpha_t)$

where α_0 is the angle between abscissa and the air gap line of the magnetizing characteristic, α_s is the angle between abscissa and the chord which initiates form the origin and passes through the operating point, and α_t is the angle between the abscissa and the tangent at the operating point.

In the conventional quasi-linear model, saturation of the magnetizing flux is taken into account by linearization process that takes the slope of the chord which emanates from the origin and passes through the operating point on the magnetizing characteristic as a saturated value of magnetizing reactance. The value is then continually adjusted as the operating changes from instant to instant[6]. This approach in often sufficiently accurate since the large signal transients as well as steady state behavior of the machine is predicted with acceptable accuracy. Moreover, small signal behavior is also predicted for the majority of

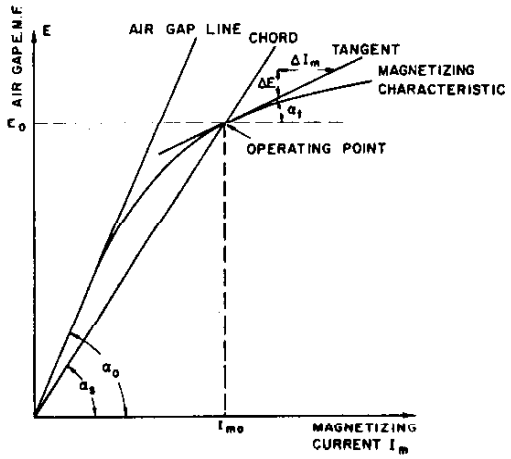

Fig. 1. Definition of magnetizing reactances.

cases in which the inherent damping of the motor is sufficiently large[4]. It is clear hovever, that changes in flux or air gap c.m.f. E, resulting from a perturbation in magnetizing current I_m, are forced to occur along the chord slope through the operating point. In an actual machine, however, changes in flux resulting from the same change in magnetizing current is clearly much smaller due to saturation. This implies that the saturated magnetizing reactance which truly exists during the dynamic process should be the instantaneous slope $x_{mt(sat)}=\Delta E/\Delta I_m$ at the operating point which is much smaller than the chord slope. It appears that such behavior has an important effect on the machine damping and stability, particularly when the system is on the verge of instability.

3. Induction Machine Transient Saturation Model

In general, incorporation of a transient saturated value of magnetizing reactance directly into a large signal induction machine model results in a set of nonlinear equations of considerable complexity since the magnetizing reactance as well as magnetizing current is a function of time. A more efficient approach is to model the magnetizing curve, Fig. 1, directly so that both small signal and large signal requirements are satisfied implicitly. In the past, modeling of induction machines has utilized d, q axis theory with great utility. Depending upon whether voltage or current is expicitly known, it has been found convenient to align either the machine terminal voltage[2] or current[7] with one of the axes of rotating d, q reference frame. The equations of transformation needed to refer system variables to the rotating frame are readily deduced since the terminal voltage or current is an independent time function. In either case, however, such manipulation of the machine equations results in a magnetizing current i_m, which has two components i_{mq} and i_{md}. These currents, in turn, result in d and q axis flux components Ψ_{mq} and Ψ_{md}. When considering the saturation of the magnetizing field, it is clearly necessary to deal with these magnetizing flux components simultaneously since saturation is caused by the instantaneous amplitude of magnetizing current (or MMF) and not by its individual components. As a result, the processing required to achieve the desired saturation effect remains complex.

It would be useful to consider means for forcing alignment of one of the d, q axes, say the d axis with the magnetizing flux Ψ_m. In this case one of the two components would be identically equal to the instantaneous flux while its orthogonal companion component would be identically zero as illustrated in the phasor diagram of Fig. 2. Hence, the saturation effect need be modeled only in the d axis while the

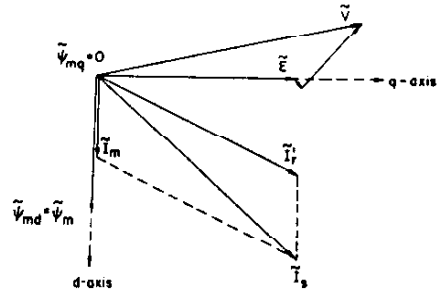

Fig. 2. Steady state phasor diagram of induction machine.

usual constant parameter model can be used in the q axis since, ideally, the flux in this axis is negligible. Such an axes orientation would clearly simplify the computation required to represent saturation.

In order to mechanize a forced alignment of the d axis with the magnetizing flux Ψ_m application of feedback control principles is useful. In particular, it can be observed from Fig. 2 that alignment is achieved when $\Psi_{mq}=0$. Hence Ψ_{mq} can be viewed as an error signal which must be dynamically zeroed as the simulation equations are solved for a particular transient. In order to realize the required dynamic alignment, a P-I regulator can be implemented directly in the machine simulation model which regulates Ψ_{mq} to zero by dynamically adjusting the alignment of the d, q axes. A block diagram depicting this procedure is shown in Fig. 3 where the quantity $T(\theta)$ expesses the transformation of stator variables to a rotating reference frame.

Because the q axis flux Ψ_{mq} is maintained at zero at all times, this component will operate near the origin of the magnetizing characteristic. It is sufficiently accurate to adopt the slope of the air gap line, i.e. unsaturated magnetizing reactance $x_{m(\mathrm{unsat})}$ as the dynamic reactance for the q axis magnetizing field. In the case of the d axis, the flux Ψ_{md} equals Ψ_m, the instantaneous amplitude of air gap flux. In general, this component of flux will be operating in the vicinity of the 'knee' of the magnetizing characteristic where saturation becomes important. The magnetizing reactance is effectively the transient value of saturated reactance $x_{m(\mathrm{sat})}$, the slope of the tangent of the magnetizing characteristic at the operating point. It can be imagined that the operating point continuously moves along the saturated region of the magnetizing characteristic during the nonlinear process. The corresponding tangent at the operating point continuously changes its slope as well. An infinity of tangents will constitute the magnetizing characteristic. Therefore it is simply necessary to incorporate the nonlinear magnetizing characteristic itself into the d axis portion of the d, q model.

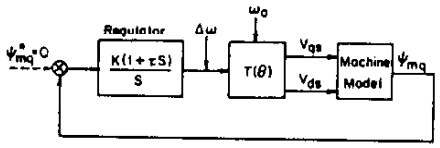

Fig. 3. Block diagram illustrating feedback scheme for axes alignment.

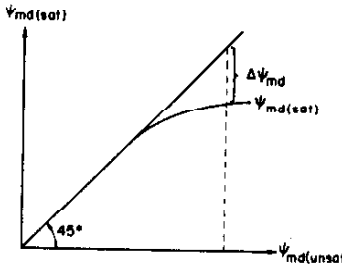

Fig. 4. Re-drawn magnetizing characteristic for the purpose of computer simulation.

Fig. 4 is a re-drawn magnetizing characteristic for the purpose of computer simulation where the abscissa is the unsaturated d axis magnetizing flux $\Psi_{md(\mathrm{unsat})}=i_{md}x_{m(\mathrm{unsat})}$ and the ordinate is the saturated d axis magnetizing flux $\Psi_{md(\mathrm{sat})}=\Psi_{md(\mathrm{unsat})}-\Delta\Psi_{md}$. The d axis stator total flux Ψ_{ds} and rotor total flux Ψ_{dr}' can then be expressed as

$$\Psi_{ds}=x_{ls}i_{ds}+\Psi_{md(\mathrm{sat})}=x_{ls}i_{ds}+[\Psi_{md(\mathrm{unsat})}-\Delta\Psi_{md}] \quad (1)$$

$$\Psi_{dr}'=x_{lr}'i_{dr}'+\Psi_{md(\mathrm{sat})}=x_{lr}'i_{dr}'+[\Psi_{md(\mathrm{unsat})}-\Delta\Psi_{md}] \quad (2)$$

The d axis stator and rotor currents can be written as

$$i_{ds}=\frac{\Psi_{ds}-\Psi_{md(\mathrm{unsat})}+\Delta\Psi_{md}}{x_{ls}} \quad (3)$$

$$i_{dr}'=\frac{\Psi_{dr}'-\Psi_{md(\mathrm{unsat})}+\Delta\Psi_{md}}{x_{lr}'} \quad (4)$$

Where x_{ls} and x_{lr}' are the stator and rotor leakage reactances. Thus, the d axis unsaturated magnetizing flux $\Psi_{md(\mathrm{unsat})}$ can be expressed

$$\Psi_{md(\mathrm{unsat})}=x_{m(\mathrm{unsat})}i_m=x_{m(\mathrm{unsat})}(i_{ds}+i_{dr}')=x_{m(\mathrm{unsat})}\left[\frac{\Psi_{ds}-\Psi_{md(\mathrm{unsat})}+\Delta\Psi_{md}}{x_{ls}}+\frac{\Psi_{dr}'-\Psi_{md(\mathrm{unsat})}+\Delta\Psi_{md}}{x_{lr}'}\right] \quad (5)$$

or

$$\Psi_{md(\mathrm{unsat})}=\frac{x_m^*}{x_{ls}}\Psi_{ds}+\frac{x_m^*}{x_{lr}'}\Psi_{dr}'+x_m^*\left(\frac{1}{x_{ls}}+\frac{1}{x_{lr}}\right)\Delta\Psi_{md} \quad (6)$$

where

$$x_m^*=\frac{1}{(1/x_{m(\mathrm{unsat})})+(1/x_{ls})+(1/x_{lr}')} \quad (7)$$

Eqs. (6) and (7) illustrate that the unsaturated value of magnetizing reactance is also used in the d

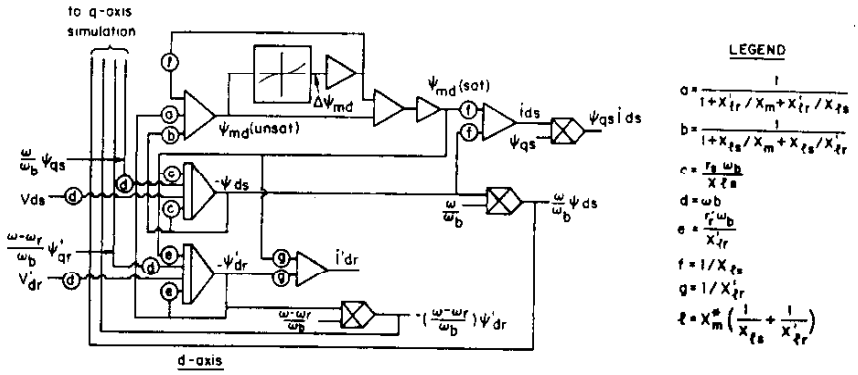

Fig. 5. Simulation diagram of the modified d axis circuit including the effect of spatially dependent saturation.

axis circuit of the saturated model but at the same time uses a nonlinear relationship $\Delta\Psi_{md}$ which expresses how much saturation exists at a given flux level.

Eqs. (3) to (7) serve to define the motor currents and air gap flux linkages in terms of the motor self flux linkages Ψ_{ds}, Ψ'_{dr} Ψ_{qs} and Ψ'_{qr}. The final step in the solution is to develop expressions for these self linkages. The stator and rotor d axis flux linkages are simply obtained from Kirchoff's Voltage Law as

$$\Psi_{ds}=\omega_b\int_0^t[v_{ds}+(\omega/\omega_b)\Psi_{qs}-r_s i_{ds}]dt \qquad (8)$$

$$\Psi'_{dr}=\omega_b\int_0^t[(\omega-\omega_r/\omega_b)\Psi'_{qr}-r'_r i'_{dr}]dt \qquad (9)$$

where the currents i_{ds} and i'_{dr} are found from Eqs. 3 and 4. Equations for the corresponding q axis flux linkages are evident by analogy.

Fig. 5 shows a simulation diagram of the modified d axis circuit which incorporates Eqs. (1) to (7). The corresponding q axis portion of the simulation diagram remains the same as that in the conventional quasi-linear model.

4. Description of System Studied

A simplified diagram of the VSI induction motor drive that has been studied with the new simulation model is shown in Fig. 6. Owing to the limitation of equipment, a typical rectifier-inverter configuration was not mechanized in this case. Rather, the rectifier portion of the drive system was replaced by a DC motor-generator set. A filter inculuding a smoothing reactor, a resistor and a capacitor; an inverter with capacitor-forced commutation circuitry and an induction motor coupled with a DC dynamometer completed the drive system. The parameters for the system are listed in the Appendix. It should be mentioned that the filter parameters were chosen to facilitate the study by exaggerating system instability and do not necessarily correspond to values encountered in a practical drive.

It seems appropriate to also discuss briefly the method of simulation of the remainder of the system components. Specifically, the DC generator was simulated by using a functional representation with its armature resistance modeled but neglecting the small armature inductance. Simulation of the filter and the inverter is discussed in reference (8). As is usual practice, the switching of the inverter was simulated without regard to the commutating circuitry. That is to say, it is assumed that commutation occurs instantaneously in the inverter. The simulation of the induction machine, which takes the spatial magnetizing flux saturation into consideration, was implemented as mentioned above and more details can be found in reference (5).

During the experiments the amplitude of the fundamental component of the open circuit inverter voltage V_s was decreased linearly with the steady state operating frequency f_e. That is to say, a constant volts-per-hertz type of operation was maintained. It is convenient to denote frequency by the frequency ratio $f_R=f_e/f_b$ where f_b is the base frequency (60 Hz)[9]. The terminal voltage V_s can then be written in the form $V_s=f_R V_m$ where V_m is the volt-per-hertz ratio at the operating point. Thus, the value of V_m can be utilized as a measure of the degree of saturation at the operating point of the machine. A unit value of volts-per-hertz ratio, which corresponds to rated voltage and

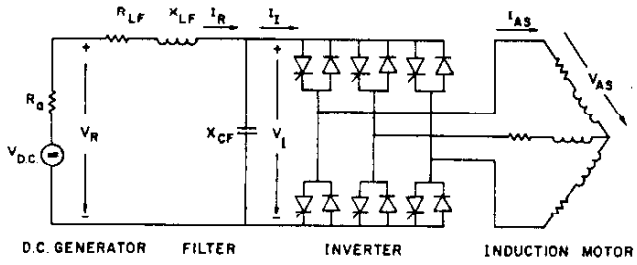

Fig. 6. System studied.

rated frequency, will be viewed as the reference for the saturation degree at the operating point.

In order to develop the proper open-circuit voltage across the machine terminals, the voltage of DC generator was set at $V_R=(\pi/2)f_R V_m$[1]. After being set for a given frequency, V_R was kept unchanged for during the loading process. The instability region was detected by increasing the load in shaft until the oscillation barely disappears. A small perturbation in load torque was then impressed to see if a sustained oscillation could take place. If so, this load was viewed as being on the boundary between stable and unstable operation. The same criterion was applied in the manipulation of the analog computer simulation as well.

5. Saturation Effects on the Stability Region

Contours of zero damping which define the instability region for the volts-per-hertz ratios $V_m=0.8$, 1.0, 1.1, are shown in Figs. 7 and 8. The instability regions are plotted in terms of frequency ratio f_R as abscissa and the per unit output torque as ordinate. For each contour the dashed line indicates the results predicted with the quasi-linear model, the dot-dashed line indicates the predicted results with the transient saturation model and the solid line shows the test results taken on an actual 7.5 HP system. From these figures, the following useful conclusions are apparent.

(1) The computed results predicted by the transient saturation model nearly coincides with the measurements for unsaturated as well as saturated conditions. This fact clearly demonstrates that the transient saturation model possesses the elusive quality needed for accurately predicting the small signal behavior (dynamics) of the VSI induction motor drive. It also reveals that the transient saturation of the magnetizing flux in one of the major factors affecting the prediction accuracy.

(2) Since the degree of saturation increases as load decreases, the entire instability region moves up and shrinks so significantly that there is no oscillation existing at no-load and light load operation. As a result, the saturation of the magnetizing flux in the motor clearly has a positive effect on the damping of a drive system. It is of interest to point out that when the machine is highly saturated, for example at $V_m=1.2$ or higher for this tested drive system, the instability region disappears entirely.

(3) With an increase of the degree of saturation of the operating point the discrepancies between the predictions made by the transient saturation model and the quasi-linear saturation model become larger and larger. At a lower degree

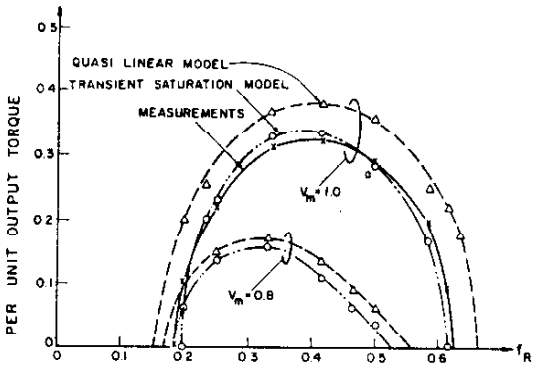

Fig. 7. Instability regions for $V_m=0.8$, 1.0.

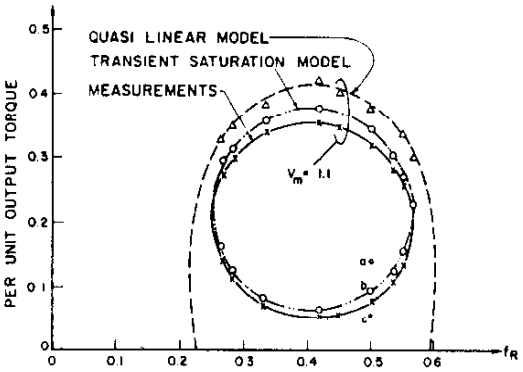

Fig. 8. Instability region for $V_m=1.1$.

of saturation ($V_m=0.8$ in Fig. 7), the difference between the computed results predicted by the two models is not so evident. This behavior is clearly because the transient saturated magnetizing reactance (the slope of the tangent of the magnetizing characteristic at the operating point) does not differ appreciably from the steady state saturated magnetizing reactance (the slope of the chord through the operating point) for an non-saturated condition. At higher saturation ($V_m=1.1$ in Fig. 8), the instability region of the drive system predicted by the quasi-linear saturation model is so much larger than that predicted by the transient saturation model as to make the drive system appear to be always unstable for no-load operation for range of frequencies.

As a verification of these observations, operation at three operating points a, b, c for $V_m=1.1$ are shown in detail in the next several figures. These points correspond to 30Hz operation, ($f_R=0.5$). Point a, which corresponds to 0.14 per unit output torque, is within the instability region of the drive system, where negative damping exists. With operation at this point, a small perturbation in torque causes an increasing system oscillation. Analog computer traces of this condition

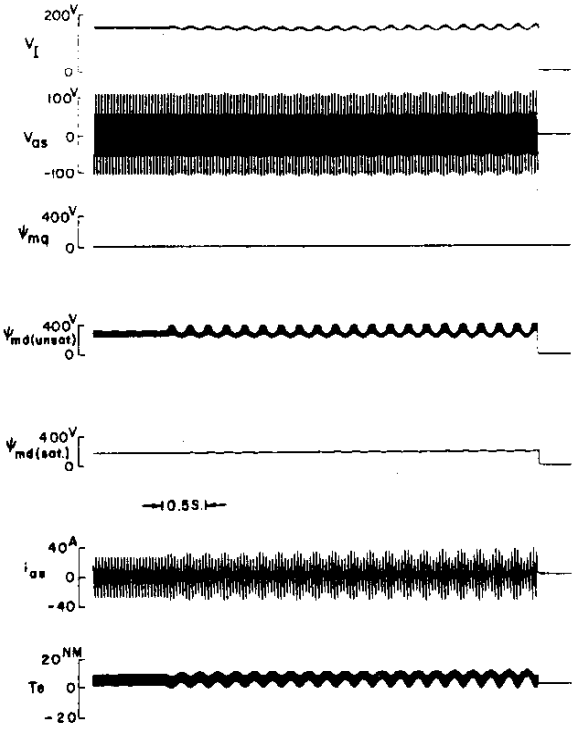

Fig. 9. Computer traces of the transient saturation model for $V_m=1.1$, $f_R=0.5$, $T_e=0.14$ (pu).

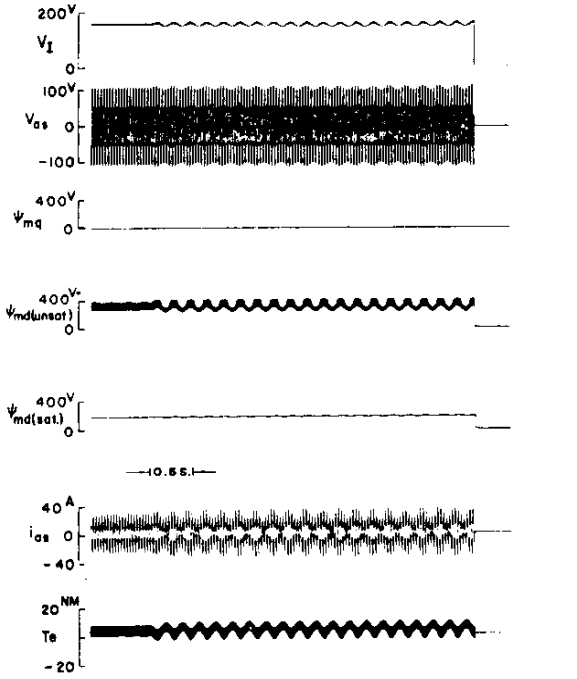

Fig. 10. Computer traces of the transient saturation model for $V_m=1.1$, $f_R=0.5$, $T_e=1.5$ (pu).

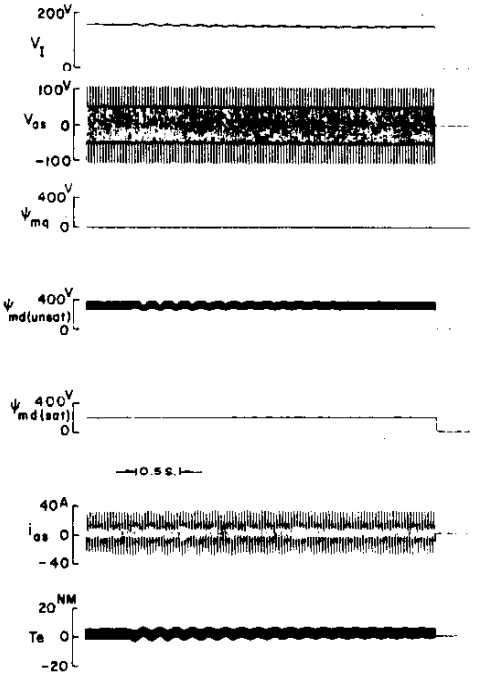

Fig. 11. Computer traces of the transient saturation model for $V_m=1.1$, $f_R=0.5$, $T_e=0.065$ (pu).

is shown in Fig. 9 using the transient saturation model. At point b, which corresponds to 0.1 per unit output torque, operation is defined at the boundary of the instability region. A small torque perturbation causes the system to produce a sustained oscillation as shown in Fig. 10. Point c, which corresponds to 0.065 per unit output torque, is outside the instability region and therefore is a stable operating point. Since positive damping exists outside the region, a small perturbation in torque, Fig. 11, causes only a damped oscillation in the system uning a dynamic type of saturation model. These traces clearly demonstrate good correlation with experiment.

It can be noted that point c is still within the instability region predicted by the quasi-linear model. Fig. 12 shows the results of a simulation of the induction machine with the quasi-linear type of saturation at point c. A very strong oscillation can be noted. This computer trace confirms that the saturation model based on conventional theory is not valid for predicting stability.

The results that have been computed in Figs. 7 and 8 have utilized an analog computer simulation which solves the nonlinear equations in detail. It is clear that a linearized form of the relevant equations could also be used for predicting the stability region and would be preferable for most studies. Other aspects of stability, however, require a full non linear model. In particular,

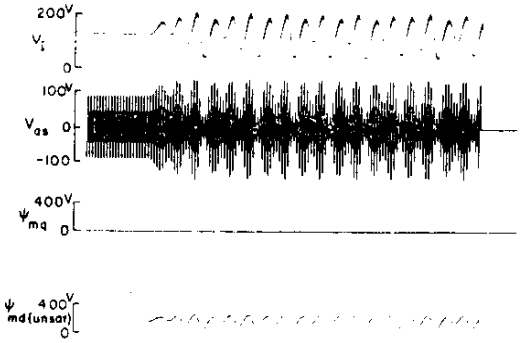

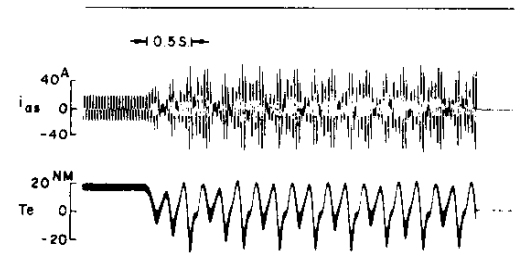

Fig. 12. Computer traces of the quasi-linear system model for $V_m=1.1$, $f_R=0.5$, $T_e=0.065$ (pu).

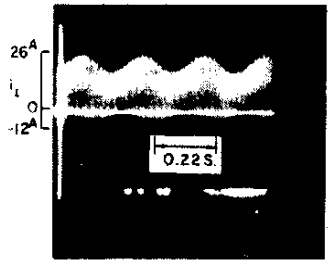

Fig. 13. Waveform of inverter current i_t for $V_m=1.0$, $f_R=0.5$, $T_e=0.284$ (pu).

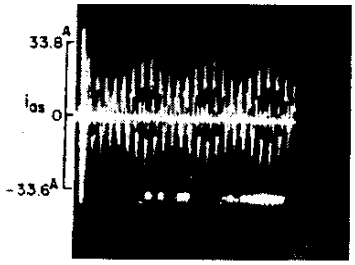

Fig. 14. Waveform of motor line current i_{as} for $V_m=1.0$, $f_R=0.5$, $T_e=0.284$ (pu).

it is often important to determine the peak to peak magnitude of the oscillation in order to specify ratings of inverter components. Figs. 13 and 14 show measurements of motor line current and inverter DC current

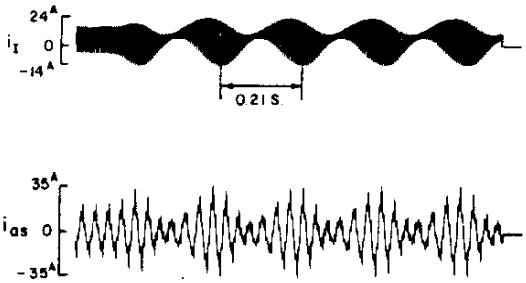

Fig. 15. Computer traces of i_t and i_{as} for $V_m=1.0$, $f_R=0.5$, $T_e=0.284$ (pu).

Table 1. Oscillation amplitude and period at point a of Fig. 7.

Quantity	Measurement	Computation
Period	0.22 s	0.21 s
Amplitude of i_t		
Positive amplitude	26 A	24 A
Negative amplitude	12 A	14.5 A
Peak to peak amplitude	38 A	38.5 A
Amplitude of i_{as}		
Positive amplitude	33.8 A	35 A
Negative amplitude	33.6 A	35 A
Peak to peak amplitude	67.4 A	70 A

taken by a digital oscilloscope of steady state operation at point a of Fig. 7. In Fig. 15 is a computer trace again computed using the transient saturation model. A tabulation of the results are given in Table 1. Very good correlation is apparent in both the oscillation period and the peak-to-peak oscillation amplitude which further substantiates the validity of the new model.

6. Conclusion

The spatial attributes of magnetizing flux saturation in an induction motor play a surprisingly important role in the stability of an inverter induction motor drive system. Saturation acts to increase system damping, especially at no-load or light load operation and significantly reduce the instability region of operation at low operating frequency. Studies of large signal dynamic behavior of an inverter drive system must therefore be carried out with a system model in which the spatially dependent saturation in the motor has been included.

References

(1) T. A. Lipo & P. C. Krause: "Stability Analysis of Rectifier-Inverter Induction Motor Drive," *IEEE Trans. Power Apparatus Syst.*, PAS-88, (1969)

(2) P. C. Krause & T. A. Lipo: "Analysis and Simplified Representations of a Rectifier-Inverter Induction Motor Drive," *ibid.*, PAS-88, 588 (1969)

(3) R. Yarema & G. Studtman: Discussion of Ref 1. *ibid.*, **PAS-88**, 63 (1969)
(4) J. A. A. Melkebeek: "Influence of Saturation on the Stability Limits of a Voltage Fed Induction Motor," Conf. Proc., 15th Universities Power Engr. Conf., University of Leicester, p. 2B2-1(1980)
(5) Y. K. He & T. A. Lipo: "Computer Simulation of an Induction Machine with Spatially Dependent Saturation", 1983 IEEE Power Engineering Society Winter Meeting, Jan. 31—Fed 5, 1983 and *IEEE Trans. Power Apparatus Syst.* (to appear)
(6) F. P. de Mello & G. W. Walsh: "Reclosing Transients in Induction Motors with Terminal Capacitors", *AIEE Trans. Power Apparatus Syst.*, **80**, 1206 (1961)
(7) T. A. Lipo & E. P. Cornell: "State-Variable Analysis of a Controlled Current Induction Motor Drive System", *IEEE Trans. Industr. Applic.*, **IA-13**, 321 (1977)
(8) L. T. Woloszyk: "An Analog Computer Study of a Static A.C. Drive System," M.S. thesis, University of Wisconin-Madison (1967)

Appendix

Nameplate data and parameters of tested VSI in duction motor drive system.

DC Generator:
5 kW 115 V 43.5 A
1,150 R.P.M.
Armature resistance $R_a = 1.7\ \Omega$ (two sets in series)

Filter:
Resistance $R_{LF} = 0.9\ \Omega$
Reactance $X_{LF} = 37\ \Omega$ (at 60 Hz)
Capacitance $x_{CF} = 1.47\ \Omega$ (at 60 Hz)

Induction Motor:
7.5 HP 208/220/440 V 21/20/10 A
1,725 R.P.M. 60 Hz three-phases
Stator: $r_s = 0.193\ \Omega$, $x_{ls} = 0.832\ \Omega$ (at 60 Hz)
Rotor: $r'_r = 0.13\ \Omega$, $x'_{lr} = 0.832\ \Omega$ (at 60 Hz)
Unsaturated magnetizing reactance
$x_{m(unsat)} = 16.25\ \Omega$ (60 Hz)

Inertia of induction motor coupled with dynamometer: $J = 0.19$ (kg-M^2)

Connecting wire and inverter equivalent resistance $r_t = 0.1\ \Omega$

Equivalent reactance of leads, inverter and dI/dt limiter $x_t = 0.01\ \Omega$ (60 Hz)

Authors

Yi-Kang He was born in China on September 22, 1941. He graduated from the Department of Electrical Engineering of Tsinghua University, Peking, China. Since graduation, he has been working at Department of Electrical Engineering of Zhejiang University, Hangzhou, China, as a Lecturer. From 1981 to 1983, he worked at the Department of Electrical and Computer Engineering in University of Wisconsin, Wisconsin, U.S.A., as a Visiting Scholar. His fields of interest include electric machines, AC drives and power electronics.

Thomas A. Lipo is currently a Professor in the Department of Electrical Engineering, University of Wisconsin, Wisconsin, U.S.A. He received the B.E.E. and M.S.E.E. degrees from Marquette University in 1962 and 1964 and the Ph.D. degree in E.E. from the University of Wisconsin in 1968. He was an N.R.C. Postdoctoral Fellow at U.M.I.S.T. in Manchester, England, during the year 1968—1969. From 1969 to 1979 he was an Electrical Engineer in the Power Electronics Laboratory of Corporate Research and Development of the General Electric Company, Schenectady, New York. While at G.E. he pioneered the computer simulation of many types of static power converter systems. He was also heavily engaged in the development of algorithms for control of solid state converter drives for which he received an IEEE prize paper award and six patents. He has contributed to the analysis and design of a wide range of industrial applications including AC drives for ball mills, pumped hydro, excavators, grinding equipment as well as traction drives for transit cars, locomotives and off highway vehicles.

Dr. Lipo is a Senior Member of IEEE and serves on the Synchronous Machine Subcommittee, the Electric Machine Theory Subcommittee, the Industrial Drives Committee and the Induction Machine Subcommittee where is a Past Chairman. Dr. Lipo has also served on the Program Committee of numerous conferences including the IEEE Power Electronics Specialists Conference for the past seven years and where he was Program Chairman in 1979. He is an Associate Editor of the Journal Electric Machines and Power Systems, and Editor of the forthcoming IEEE Journal of Power Electronics. He has authored or co-authored over fifty technical papers.

WEMPEC

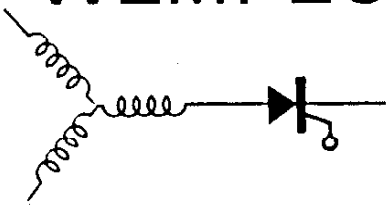

Wisconsin Electric Machines and Power Electronics Consortium

RESEARCH REPORT
82-13

Saturation Effects in the Stability Analysis of a VSI Induction Motor Drive

Yi-Kang He and T.A. Lipo
University of Wisconsin
Madison, Wisconsin, U.S.A.

Department of Electrical and Computer Engineering
University of Wisconsin-Madison
Madison, Wisconsin 53706

December 1982

Paper

UDC 621.313.333.016.352 : [621.314.57 : 621.311.69]

Saturation Effects in the Stability Analysis of a VSI Induction Motor Drive

By

Yi-Kang He Non-member T. A. Lipo Non-member

Summary

A computer model of a saturated induction mcchine is introduced which takes into account the effect of spatially dependent main-flux saturation. The approach is used to model a voltage source inverter (VSI) drive and the instability region of such a drive system is predicted with the new saturation model. Comparison of the results computed by the new model with both tested results and computed results predicted by the conventional quasi-linear model indicate surprisingly important effects of saturation on the small as well as large signal behavior (transients) of a drive system. Discrepancies which have long existed between theory and practice concerning the prediction of dynamic instability of VSI drive by the small signal theory are resolved.

1. Introduction

Due to its widespread application the voltage source inverter (VSI) fed induction motor drive is a very important class of AC frequency variable drive. Since a stepped wave voltage is supplied to the motor there are many new features and corresponding new problems associated with this type of drive. One important such problem is the instability that occurs at low frequency due to the interchange of energy between its DC link filter components and magnetic field and rotor of the machine. Many application opportunities demand operation over a wide speed range, particularly low speed operation. Therefore, the problem of system instability at low operating frequencies is a major concern in the design of VSI induction motor drive.

In the past, considerable work has been devoted to the analysis of VSI drives and models have been developed to predict dynamic behavior[1][2]. These models have been successfully used to predict the instability phenomenon of a drive system and to identify the trend of the instability region with changes in system parameters. However, there is no denying the fact that in some cases the theoretical prediction still does not correlate well with practical measurements. In general, it has been observed that the predicted instability region is usually larger than the measurement and the added damping has been attributed to inverter losses which are not included in the usual analysis[3]. Instability is typically predicted to occur over a range of no load conditions and to persist up to a particular load condition. The predicted instability region takes on the form of a half-oval with the widest portion of the instability range occuring at no load[1]. On the other hand, test results often indicate that the no load condition is stable and the motor must be loaded before instability can occur[3]. Oscillations begin to appear as the load is increased and are sustained over a range of load. When the load is increased beyond a certain point the amplitude of the oscillation is observed to decrease until at heavy load the oscillation again disappears. It appears that this phenomenon cannot be predicted by classical models even with conventional models of saturation.

Recently, however, a new small signal computer model of a saturated induction machine has been developed which takes into consideration the spatial dependence on main flux saturation[4]. The authors have extended this model to portray large signal transients as well a small signal dynamics[5]. Using this new model, the instability region obtained by inserting additional resistances in series with stator of

Yi-Kang He was & *T. A. Lipo* is with Departmemt of Electrical and Computer Engineering, University of Wisconsin-Madison, U. S. A. Manuscript received Feb., 17, 1983.

sinusoidally excited induction machine was predicted with extraordinary accuracy. The purpose of this paper is to extend this new analytical model to the study of induction motor drives and, in particular, to improve the prediction of the instability region for a VSI induction motor drive system.

2. Concept of Transient Saturation

In order to illustrate the concept of transient saturation and its influence on stability, a typical magnetizing characteristic of an induction machine is shown in Fig. 1. Along this magnetizing characteristic, three magnetizing reactances can be defined, namely

Unsaturated magnetizing reactance:

$x_{m(\mathrm{unsat})}=\tan(\alpha_o)$

Steady state saturated magnetizing reactance:

$x_{m(\mathrm{sat})}=\tan(\alpha_s)$

Transient saturated magnetizing reactance:

$x_{mt(\mathrm{sat})}=\tan(\alpha_t)$

where α_o is the angle between abscissa and the air gap line of the magnetizing characteristic, α_s is the angle between abscissa and the chord which initiates form the origin and passes through the operating point, and α_t is the angle between the abscissa and the tangent at the operating point.

In the conventional quasi-linear model, saturation of the magnetizing flux is taken into account by linearization process that takes the slope of the chord which emanates from the origin and passes through the operating point on the magnetizing characteristic as a saturated value of magnetizing reactance. The value is then continually adjusted as the operating changes from instant to instant[6]. This approach in often sufficiently accurate since the large signal transients as well as steady state behavior of the machine is predicted with acceptable accuracy. Moreover, small signal behavior is also predicted for the majority of

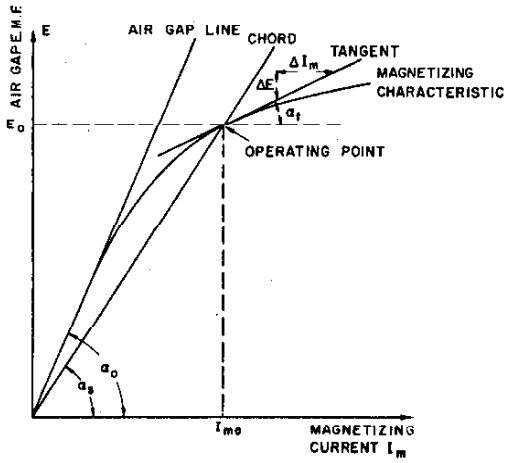

Fig. 1. Definition of magnetizing reactances.

cases in which the inherent damping of the motor is sufficiently large[4]. It is clear hovever, that changes in flux or air gap e.m.f. E, resulting from a perturbation in magnetizing current I_m, are forced to occur along the chord slope through the operating point. In an actual machine, however, changes in flux resulting from the same change in magnetizing current is clearly much smaller due to saturation. This implies that the saturated magnetizing reactance which truly exists during the dynamic process should be the instantaneous slope $x_{mt(\mathrm{sat})}=\Delta E/\Delta I_m$ at the operating point which is much smaller than the chord slope. It appears that such behavior has an important effect on the machine damping and stability, particularly when the system is on the verge of instability.

3. Induction Machine Transient Saturation Model

In general, incorporation of a transient saturated value of magnetizing reactance directly into a large signal induction machine model results in a set of nonlinear equations of considerable complexity since the magnetizing reactance as well as magnetizing current is a function of time. A more efficient approach is to model the magnetizing curve, Fig. 1, directly so that both small signal and large signal requirements are satisfied implicitly. In the past, modeling of induction machines has utilized d, q axis theory with great utility. Depending upon whether voltage or current is expicitly known, it has been found convenient to align either the machine terminal voltage[2] or current[7] with one of the axes of rotating d, q reference frame. The equations of transformation needed to refer system variables to the rotating frame are readily deduced since the terminal voltage or current is an independent time function. In either case, however, such manipulation of the machine equations results in a magnetizing current i_m, which has two components i_{mq} and i_{md}. These currents, in turn, result in d and q axis flux components Ψ_{mq} and Ψ_{md}. When considering the saturation of the magnetizing field, it is clearly necessary to deal with these magnetizing flux components simultaneously since saturation is caused by the instantaneous amplitude of magnetizing current (or MMF) and not by its individual components. As a result, the processing required to achieve the desired saturation effect remains complex.

It would be useful to consider means for forcing alignment of one of the d, q axes, say the d axis with the magnetizing flux Ψ_m. In this case one of the two components would be identically equal to the instantaneous flux while its orthogonal companion component would be identically zero as illustrated in the phasor diagram of Fig. 2. Hence, the saturation effect need be modeled only in the d axis while the

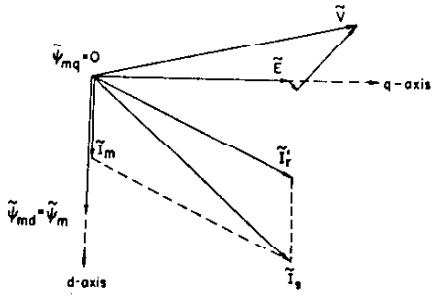

Fig. 2. Steady state phasor diagram of induction machine.

usual constant parameter model can be used in the q axis since, ideally, the flux in this axis is negligible. Such an axes orientation would clearly simplify the computation required to represent saturation.

In order to mechanize a forced alignment of the d axis with the magnetizing flux Ψ_m application of feedback control principles is useful. In particular, it can be observed from Fig. 2 that alignment is achieved when $\Psi_{mq}=0$. Hence Ψ_{mq} can be viewed as an error signal which must be dynamically zeroed as the simulation equations are solved for a particular transient. In order to realize the required dynamic alignment, a P-I regulator can be implemented directly in the machine simulation model which regulates Ψ_{mq} to zero by dynamically adjusting the alignment of the d, q axes. A block diagram depicting this procedure is shown in Fig. 3 where the quantity $T(\theta)$ expesses the transformation of stator variables to a rotating reference frame.

Because the q axis flux Ψ_{mq} is maintained at zero at all times, this component will operate near the origin of the magnetizing characteristic. It is sufficiently accurate to adopt the slope of the air gap line, i.e. unsaturated magnetizing reactance $x_{m(\mathrm{unsat})}$ as the dynamic reactance for the q axis magnetizing field. In the case of the d axis, the flux Ψ_{md} equals Ψ_m, the instantaneous amplitude of air gap flux. In general, this component of flux will be operating in the vicinity of the 'knee' of the magnetizing characteristic where saturation becomes important. The magnetizing reactance is effectively the transient value of saturated reactance $x_{m(\mathrm{sat})}$, the slope of the tangent of the magnetizing characteristic at the operating point. It can be imagined that the operating point continuously moves along the saturated region of the magnetizing characteristic during the nonlinear process. The corresponding tangent at the operating point continuously changes its slope as well. An infinity of tangents will constitute the magnetizing characteristic. Therefore it is simply necessary to incorporate the nonlinear magnetizing characteristic itself into the d axis portion of the d, q model.

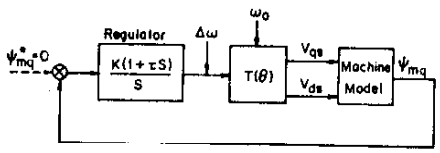

Fig. 3. Block diagram illustrating feedback scheme for axes alignment.

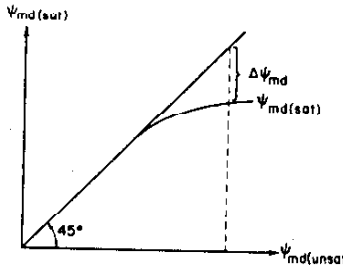

Fig. 4. Re-drawn magnetizing characteristic for the purpose of computer simulation.

Fig. 4 is a re-drawn magnetizing characteristic for the purpose of computer simulation where the abscissa is the unsaturated d axis magnetizing flux $\Psi_{md(\mathrm{unsat})}=i_{md}x_{m(\mathrm{unsat})}$ and the ordinate is the saturated d axis magnetizing flux $\Psi_{md(\mathrm{sat})}=\Psi_{md(\mathrm{unsat})}-\Delta\Psi_{md}$. The d axis stator total flux Ψ_{ds} and rotor total flux Ψ'_{dr} can then be expressed as

$$\begin{aligned}\Psi_{ds}&=x_{ls}i_{ds}+\Psi_{md(\mathrm{sat})}\\&=x_{ls}i_{ds}+[\Psi_{md(\mathrm{unsat})}-\Delta\Psi_{md}]\end{aligned}\qquad(1)$$

$$\begin{aligned}\Psi'_{dr}&=x'_{lr}i'_{dr}+\Psi_{md(\mathrm{sat})}\\&=x'_{lr}i'_{dr}+[\Psi_{md(\mathrm{unsat})}-\Delta\Psi_{md}]\end{aligned}\qquad(2)$$

The d axis stator and rotor currents can be written as

$$i_{ds}=\frac{\Psi_{ds}-\Psi_{md(\mathrm{unsat})}+\Delta\Psi_{md}}{x_{ls}}\qquad(3)$$

$$i'_{dr}=\frac{\Psi'_{dr}-\Psi_{md(\mathrm{unsat})}+\Delta\Psi_{md}}{x'_{lr}}\qquad(4)$$

Where x_{ls} and x'_{lr} are the stator and rotor leakage reactances. Thus, the d axis unsaturated magnetizing flux $\Psi_{md(\mathrm{unsat})}$ can be expressed

$$\begin{aligned}\Psi_{md(\mathrm{unsat})}&=x_{m(\mathrm{unsat})}i_m=x_{m(\mathrm{unsat})}(i_{ds}+i'_{dr})\\&=x_{m(\mathrm{unsat})}\left[\frac{\Psi_{ds}-\Psi_{md(\mathrm{unsat})}+\Delta\Psi_{md}}{x_{ls}}\right.\\&\quad\left.+\frac{\Psi'_{dr}-\Psi_{md(\mathrm{unsat})}+\Delta\Psi_{md}}{x'_{lr}}\right]\end{aligned}\qquad(5)$$

or

$$\begin{aligned}\Psi_{md(\mathrm{unsat})}&=\frac{x_m^*}{x_{ls}}\Psi_{ds}+\frac{x_m^*}{x'_{lr}}\Psi'_{dr}\\&\quad+x_m^*\left(\frac{1}{x_{ls}}+\frac{1}{x_{lr}}\right)\Delta\Psi_{md}\end{aligned}\qquad(6)$$

where

$$x_m^*=\frac{1}{(1/x_{m(\mathrm{unsat})})+(1/x_{ls})+(1/x'_{lr})}\qquad(7)$$

Eqs. (6) and (7) illustrate that the unsaturated value of magnetizing reactance is also used in the d

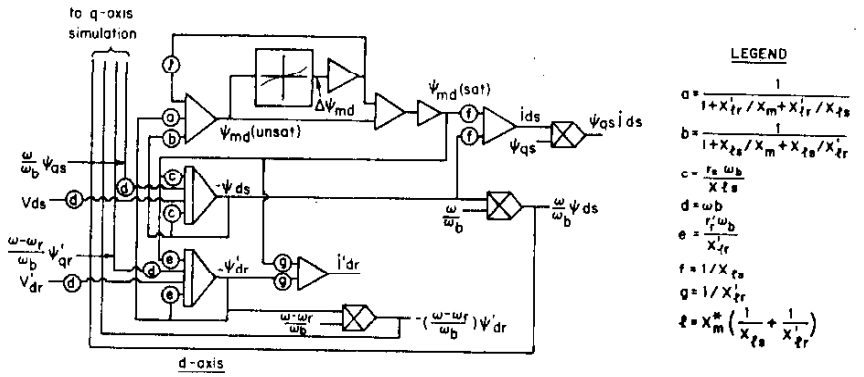

Fig. 5. Simulation diagram of the modified d axis circuit including the effect of spatially dependent saturation.

axis circuit of the saturated model but at the same time uses a nonlinear relationship $\Delta\Psi_{md}$ which expresses how much saturation exists at a given flux level.

Eqs. (3) to (7) serve to define the motor currents and air gap flux linkages in terms of the motor self flux linkages Ψ_{ds}, Ψ'_{dr}, Ψ_{qs} and Ψ'_{qr}. The final step in the solution is to develop expressions for these self linkages. The stator and rotor d axis flux linkages are simply obtained from Kirchoff's Voltage Law as

$$\Psi_{ds}=\omega_b\int_0^t[v_{ds}+(\omega/\omega_b)\Psi_{qs}-r_s i_{ds}]dt \qquad (8)$$

$$\Psi'_{dr}=\omega_b\int_0^t[(\omega-\omega_r/\omega_b)\Psi'_{qr}-r'_r i'_{dr}]dt \qquad (9)$$

where the currents i_{ds} and i'_{dr} are found from Eqs. 3 and 4. Equations for the corresponding q axis flux linkages are evident by analogy.

Fig. 5 shows a simulation diagram of the modified d axis circuit which incorporates Eqs. (1) to (7). The corresponding q axis portion of the simulation diagram remains the same as that in the conventional quasi-linear model.

4. Description of System Studied

A simplified diagram of the VSI induction motor drive that has been studied with the new simulation model is shown in Fig. 6. Owing to the limitation of equipment, a typical rectifier-inverter configuration was not mechanized in this case. Rather, the rectifier portion of the drive system was replaced by a DC motor-generator set. A filter inculuding a smoothing reactor, a resistor and a capacitor; an inverter with capacitor-forced commutation circuitry and an induction motor coupled with a DC dynamometer completed the drive system. The parameters for the system are listed in the Appendix. It should be mentioned that the filter parameters were chosen to facilitate the study by exaggerating system instability and do not necessarily correspond to values encountered in a practical drive.

It seems appropriate to also discuss briefly the method of simulation of the remainder of the system components. Specifically, the DC generator was simulated by using a functional representation with its armature resistance modeled but neglecting the small armature inductance. Simulation of the filter and the inverter is discussed in reference (8). As is usual practice, the switching of the inverter was simulated without regard to the commutating circuitry. That is to say, it is assumed that commutation occurs instantaneously in the inverter. The simulation of the induction machine, which takes the spatial magnetizing flux saturation into consideration, was implemented as mentioned above and more details can be found in reference (5).

During the experiments the amplitude of the fundamental component of the open circuit inverter voltage V_s was decreased linearly with the steady state operating frequency f_e. That is to say, a constant volts-per-hertz type of operation was maintained. It is convenient to denote frequency by the frequency ratio $f_R=f_e/f_b$ where f_b is the base frequency (60 Hz)[1]. The terminal voltage V_s can then be written in the form $V_s=f_R V_m$ where V_m is the volt-per-hertz ratio at the operating point. Thus, the value of V_m can be utilized as a measure of the degree of saturation at the operating point of the machine. A unit value of volts-per-hertz ratio, which corresponds to rated voltage and

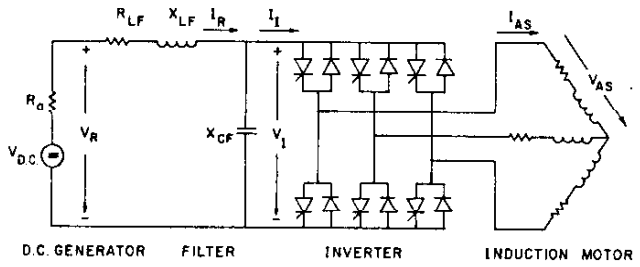

Fig. 6. System studied.

rated frequency, will be viewed as the reference for the saturation degree at the operating point.

In order to develop the proper open-circuit voltage across the machine terminals, the voltage of DC generator was set at $V_R=(\pi/2)f_R V_m$[1]. After being set for a given frequency, V_R was kept unchanged for during the loading process. The instability region was detected by increasing the load in shaft until the oscillation barely disappears. A small perturbation in load torque was then impressed to see if a sustained oscillation could take place. If so, this load was viewed as being on the boundary between stable and unstable operation. The same criterion was applied in the manipulation of the analog computer simulation as well.

5. Saturation Effects on the Stability Region

Contours of zero damping which define the instability region for the volts-per-hertz ratios $V_m=0.8$, 1.0, 1.1, are shown in Figs. 7 and 8. The instability regions are plotted in terms of frequency ratio f_R as abscissa and the per unit output torque as ordinate. For each contour the dashed line indicates the results predicted with the quasi-linear model, the dot-dashed line indicates the predicted results with the transient saturation model and the solid line shows the test results taken on an actual 7.5 HP system. From these figures, the following useful conclusions are apparent.

(1) The computed results predicted by the transient saturation model nearly coincides with the measurements for unsaturated as well as saturated conditions. This fact clearly demonstrates that the transient saturation model possesses the elusive quality needed for accurately predicting the small signal behavior (dynamics) of the VSI induction motor drive. It also reveals that the transient saturation of the magnetizing flux in one of the major factors affecting the prediction accuracy.

(2) Since the degree of saturation increases as load decreases, the entire instability region moves up and shrinks so significantly that there is no oscillation existing at no-load and light load operation. As a result, the saturation of the magnetizing flux in the motor clearly has a positive effect on the damping of a drive system. It is of interest to point out that when the machine is highly saturated, for example at $V_m=1.2$ or higher for this tested drive system, the instability region disappears entirely.

(3) With an increase of the degree of saturation of the operating point the discrepancies between the predictions made by the transient saturation model and the quasi-linear saturation model become larger and larger. At a lower degree of saturation ($V_m=0.8$ in Fig. 7), the difference between the computed results predicted by the two models is not so evident. This behavior is clearly because the transient saturated magnetizing reactance (the slope of the tangent of the magnetizing characteristic at the operating point) does not differ appreciably from the steady state saturated magnetizing reactance (the slope of the chord through the operating point) for an non-saturated condition. At higher saturation ($V_m=1.1$ in Fig. 8), the instability region of the drive system predicted by the quasi-linear saturation model is so much larger than that predicted by the transient saturation model as to make the drive system appear to be always unstable for no-load operation for range of frequencies.

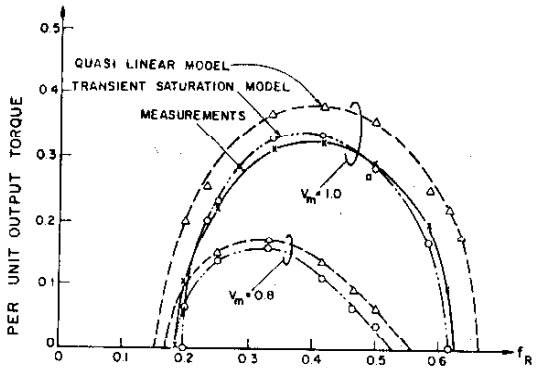

Fig. 7. Instability regions for $V_m=0.8$, 1.0.

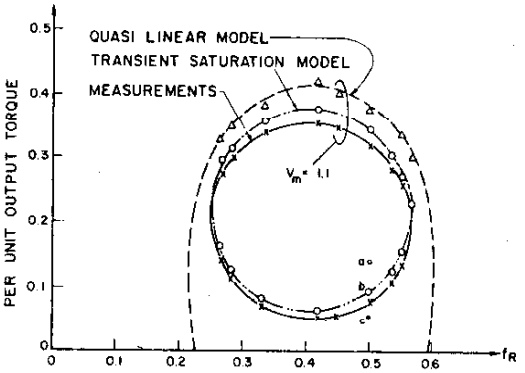

Fig. 8. Instability region for $V_m=1.1$.

As a verification of these observations, operation at three operating points a, b, c for $V_m=1.1$ are shown in detail in the next several figures. These points correspond to 30Hz operation, ($f_R=0.5$). Point a, which corresponds to 0.14 per unit output torque, is within the instability region of the drive system, where negative damping exists. With operation at this point, a small perturbation in torque causes an increasing system oscillation. Analog computer traces of this condition

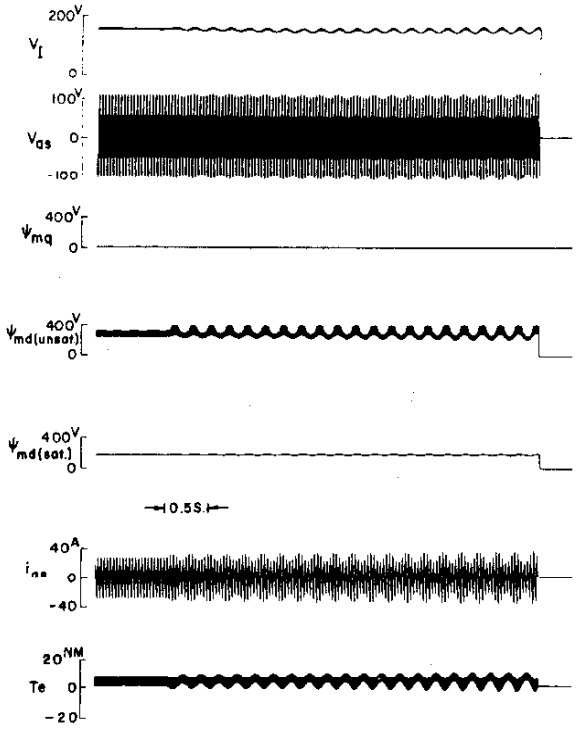

Fig. 9. Computer traces of the transient saturation model for $V_m=1.1$, $f_R=0.5$, $T_e=0.14$ (pu).

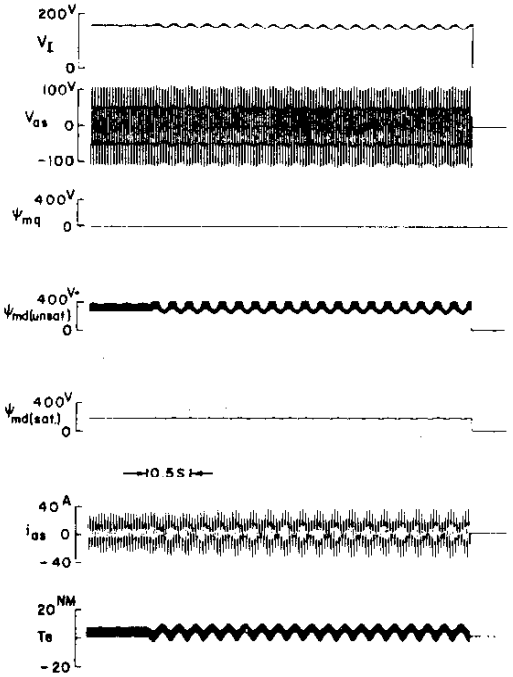

Fig. 10. Computer traces of the transient saturation model for $V_m=1.1$, $f_R=0.5$, $T_e=1.5$ (pu).

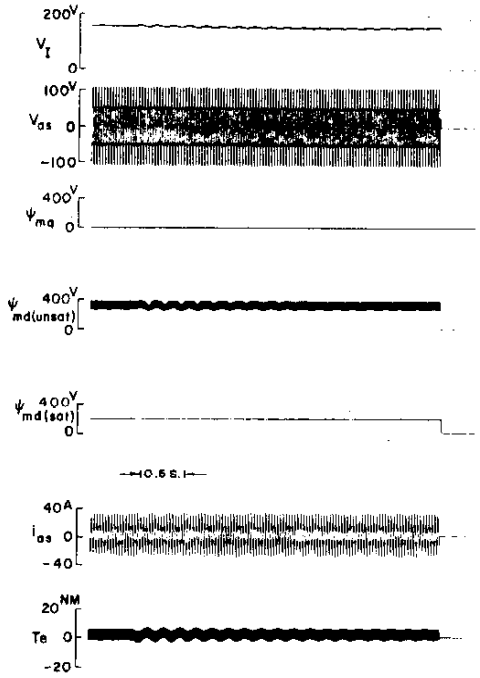

Fig. 11. Computer traces of the transient saturation model for $V_m=1.1$, $f_R=0.5$, $T_e=0.065$ (pu).

is shown in Fig. 9 using the transient saturation model. At point b, which corresponds to 0.1 per unit output torque, operation is defined at the boundary of the instability region. A small torque perturbation causes the system to produce a sustained oscillation as shown in Fig. 10. Point c, which corresponds to 0.065 per unit output torque, is outside the instability region and therefore is a stable operating point. Since positive damping exists outside the region, a small perturbation in torque, Fig. 11, causes only a damped oscillation in the system uning a dynamic type of saturation model. These traces clearly demonstrate good correlation with experiment.

It can be noted that point c is still within the instability region predicted by the quasi-linear model. Fig. 12 shows the results of a simulation of the induction machine with the quasi-linear type of saturation at point c. A very strong oscillation can be noted. This computer trace confirms that the saturation model based on conventional theory is not valid for predicting stability.

The results that have been computed in Figs. 7 and 8 have utilized an analog computer simulation which solves the nonlinear equations in detail. It is clear that a linearized form of the relevant equations could also be used for predicting the stability region and would be preferable for most studies. Other aspects of stability, however, require a full non linear model. In particular,

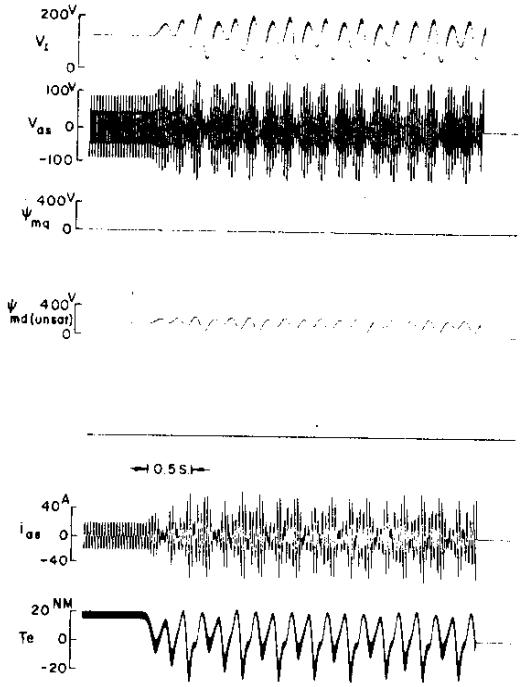

Fig. 12. Computer traces of the quasi-linear system model for $V_m=1.1$, $f_R=0.5$, $T_e=0.065$ (pu).

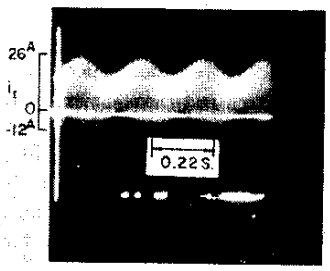

Fig. 13. Waveform of inverter current i_t for $V_m=1.0$, $f_R=0.5$, $T_e=0.284$ (pu).

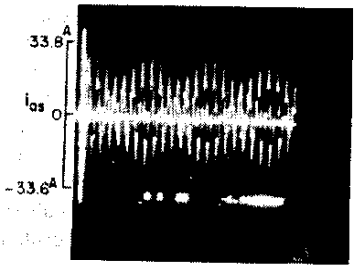

Fig. 14. Waveform of motor line current i_{as} for $V_m=1.0$, $f_R=0.5$, $T_e=0.284$ (pu).

it is often important to determine the peak to peak magnitude of the oscillation in order to specify ratings of inverter components. Figs. 13 and 14 show measurements of motor line current and inverter DC current

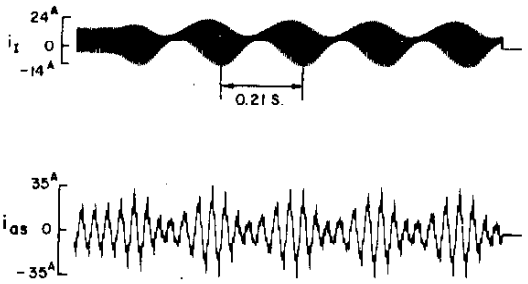

Fig. 15. Computer traces of i_t and i_{as} for $V_m=1.0$, $f_R=0.5$, $T_e=0.284$ (pu).

Table 1. Oscillation amplitude and period at point a of Fig. 7.

Quantity	Measurement	Computation
Period	0.22 s	0.21 s
Amplitude of i_t		
Positive amplitude	26 A	24 A
Negative amplitude	12 A	14.5 A
Peak to peak amplitude	38 A	38.5 A
Amplitude of i_{as}		
Positive amplitude	33.8 A	35 A
Negative amplitude	33.6 A	35 A
Peak to peak amplitude	67.4 A	70 A

taken by a digital oscilloscope of steady state operation at point a of Fig. 7. In Fig. 15 is a computer trace again computed using the transient saturation model. A tabulation of the results are given in Table 1. Very good correlation is apparent in both the oscillation period and the peak-to-peak oscillation amplitude which further substantiates the validity of the new model.

6. Conclusion

The spatial attributes of magnetizing flux saturation in an induction motor play a surprisingly important role in the stability of an inverter induction motor drive system. Saturation acts to increase system damping, especially at no-load or light load operation and significantly reduce the instability region of operation at low operating frequency. Studies of large signal dynamic behavior of an inverter drive system must therefore be carried out with a system model in which the spatially dependent saturation in the motor has been included.

References

(1) T. A. Lipo & P. C. Krause: "Stability Analysis of Rectifier-Inverter Induction Motor Drive," *IEEE Trans. Power Apparatus Syst.*, **PAS-88**, (1969)

(2) P. C. Krause & T. A. Lipo: "Analysis and Simplified Representations of a Rectifier-Inverter Induction Motor Drive," *ibid.*, **PAS-88**, 588 (1969)

(3) R. Yarema & G. Studtman: Discussion of Ref 1. *ibid.*, **PAS-88**, 63 (1969)
(4) J. A. A. Melkebeek: "Influence of Saturation on the Stability Limits of a Voltage Fed Induction Motor," Conf. Proc., 15th Universities Power Engr. Conf., University of Leicester, p. 2B2-1 (1980)
(5) Y. K. He & T. A. Lipo: "Computer Simulation of an Induction Machine with Spatially Dependent Saturation", 1983 IEEE Power Engineering Society Winter Meeting, Jan. 31—Fed 5, 1983 and *IEEE Trans. Power Apparatus Syst.* (to appear)
(6) F. P. de Mello & C. W. Walsh: "Reclosing Transients in Induction Motors with Terminal Capacitors", *AIEE Trans. Power Apparatus Syst.*, **80**, 1206 (1961)
(7) T. A. Lipo & E. P. Cornell: "State-Variable Analysis of a Controlled Current Induction Motor Drive System", *IEEE Trans. Industr. Applic.*, **IA-13**, 321 (1977)
(8) L. T. Woloszyk: "An Analog Computer Study of a Static A.C. Drive System," M.S. thesis, University of Wisconin-Madison (1967)

Appendix

Nameplate data and parameters of tested VSI in duction motor drive system.

DC Generator:
5 kW 115 V 43.5 A
1,150 R.P.M.
Armature resistance $R_a = 1.7\ \Omega$ (two sets in series)

Filter:
Resistance $R_{LF} = 0.9\ \Omega$
Reactance $X_{LF} = 37\ \Omega$ (at 60 Hz)
Capacitance $x_{CF} = 1.47\ \Omega$ (at 60 Hz)

Induction Motor:
7.5 HP 208/220/440 V 21/20/10 A
1,725 R.P.M. 60 Hz three-phases
Stator: $r_s = 0.193\ \Omega$, $x_{ls} = 0.832\ \Omega$ (at 60 Hz)
Rotor: $r_r' = 0.13\ \Omega$, $x_{lr}' = 0.832\ \Omega$ (at 60 Hz)
Unsaturated magnetizing reactance
$x_{m(\text{unsat})} = 16.25\ \Omega$ (60 Hz)

Inertia of induction motor coupled with dynamometer: $J = 0.19$ (kg-M^2)

Connecting wire and inverter equivalent resistance $r_l = 0.1\ \Omega$

Equivalent reactance of leads, inverter and dI/dt limiter $x_l = 0.01\ \Omega$ (60 Hz)

Authors

Yi-Kang He was born in China on September 22, 1941. He graduated from the Department of Electrical Engineering of Tsinghua University, Peking, China. Since graduation, he has been working at Department of Electrical Engineering of Zhejiang University, Hangzhou, China, as a Lecturer. From 1981 to 1983, he worked at the Department of Electrical and Computer Engineering in University of Wisconsin, Wisconsin, U.S.A., as a Visiting Scholar. His fields of interest include electric machines, AC drives and power electronics.

Thomas A. Lipo is currently a Professor in the Department of Electrical Engineering, University of Wisconsin, Wisconsin, U.S.A. He received the B.E.E. and M.S.E.E. degrees from Marquette University in 1962 and 1964 and the Ph.D. degree in E.E. from the University of Wisconsin in 1968. He was an N.R.C. Postdoctoral Fellow at U.M.I.S.T. in Manchester, England, during the year 1968—1969. From 1969 to 1979 he was an Electrical Engineer in the Power Electronics Laboratory of Corporate Research and Development of the General Electric Company, Schenectady, New York. While at G.E. he pioneered the computer simulation of many types of static power converter systems. He was also heavily engaged in the development of algorithms for control of solid state converter drives for which he received an IEEE prize paper award and six patents. He has contributed to the analysis and design of a wide range of industrial applications including AC drives for ball mills, pumped hydro, excavators, grinding equipment as well as traction drives for transit cars, locomotives and off highway vehicles.

Dr. Lipo is a Senior Member of IEEE and serves on the Synchronous Machine Subcommittee, the Electric Machine Theory Subcommittee, the Industrial Drives Committee and the Induction Machine Subcommittee where is a Past Chairman. Dr. Lipo has also served on the Program Committee of numerous conferences including the IEEE Power Electronics Specialists Conference for the past seven years and where he was Program Chairman in 1979. He is an Associate Editor of the Journal Electric Machines and Power Systems. and Editor of the forthcoming IEEE Journal of Power Electronics. He has authored or co-authored over fifty technical papers.